

# Relationship between damage of levee and its resonant frequency in Shinano River subjected to Niigata Chuetsu Earthquake in 2004

Toshiyuki Takahara (*Dept. of Civil Engineering, Kanazawa University, Japan*)  
Toshihide Sugimoto (*MLIT Hokuriku Regional Development Bureau, Japan*)

**Abstract** At the Niigata Chuetsu Earthquake in 2004, the levees along the Shinano River and the Uono River were widely damaged. The damage of levees depends not only on the distance from the epicenter but also on the foundation stratum of levee. In this study, we classified the degree of the damage of the levee situated 2 to 50km from the epicenter, and compared these damages with the geological categorization of the levee foundation. To make clear the seismic characteristics of each geological category, we carried out the linear elastic analysis based on multiple reflection theory using results of standard penetration and laboratory soil tests. We compared damage type with the dominant frequency by multiple reflection theory and averaged layers.

**Keywords** Niigata Chuetsu Earthquake in 2004, Levee, Seismic Characteristics, Dominant Frequency, Multiple Reflection Theory

## 1. Introduction

The Niigata Chuetsu Earthquake of inland strong earthquake occurred on 23rd Oct. 2004, its magnitude is 6.8 and depth of seismic center is 13km. The maximum magnitude of acceleration of main shock is 818 gal and three big aftershocks took place within 40 minutes after the main shock. The magnitudes of aftershocks were 6.3, 6.0 and 6.5.

The levees along the Shinano River and the Uono River were widely damaged at the earthquake and the damages of levee observed at 137 places in total. Eighty eight percent (120 places) of stricken levees were minor faults, Other 17 places were suffered from serious damage. The serious damages were distributed to 40km from epicenter.

The preliminary study suggests that the damage of levees depends not only on the distance from the epicenter, but also the foundation stratum of levee. In this study, we classified the degree of the damage into four patterns, and compared these damages with the five geological categorizations of the levee foundation. As mentioned before, the geological features may concerned with damage pattern at earthquake, however, the stochastic studies does not supply sufficient relationship. This means only geology is not enough for explanation of damage properties, and then we calculated the dominant frequency of each damaged levee using detail inspection results performed by MLIT.

## 2. Geology around Shinano River and damage types

The foundation stratum along Shinano and Uono Rivers are categorized into the five regions in geologically, which are named First and Second Floodplain Area, Alluvial Fan Area, Inclosed Meander Area of the Shinano River and Alluvial Fan Area of the Uono River located on footwall of the active fault. The geological profile along Shinano River to Uono River is shown in Fig. 1 and its legend is shown in table 1.

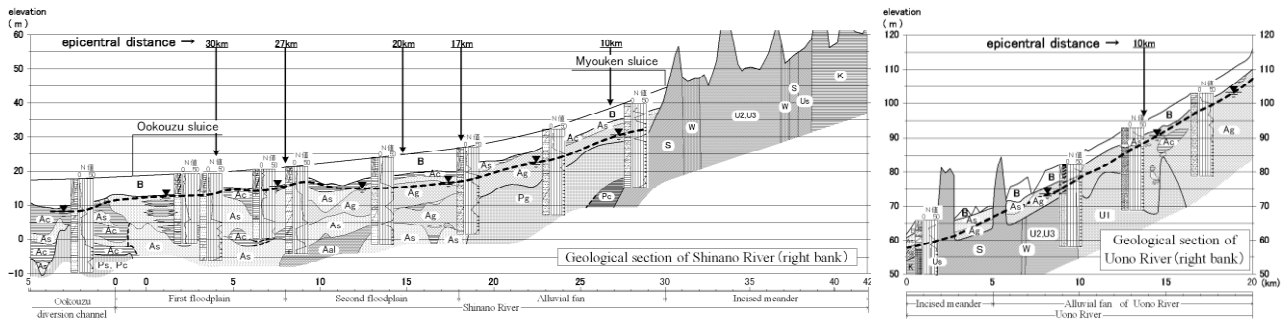


Fig.1 Longitudinal geological profile along Shinano River to Uono River.

Table 1 Legend of geological symbols In Fig. 1.

Geochronologic division	Geological classification	symbol	
Recent	banking	B	
Quaternary	Holocene	cohesive soil	Ac
		sandy soil	As
		gravelly soil	Ag
	Pleistocene	alternation of strata sand and clay	Aal
		silt + sand + gravel	U2,U3
		mudstone	Pc
Neogene	Pliocene	gravel + silt + sand	U1
		sandstone	W
		sandy mudstone + argillaceous sandstone	S
		blocky mudstone	Us
		alternation of strata sandstone and mudstone	K
		gravelly soil	Pg
mudstone and sandstone	Pc,Pg		

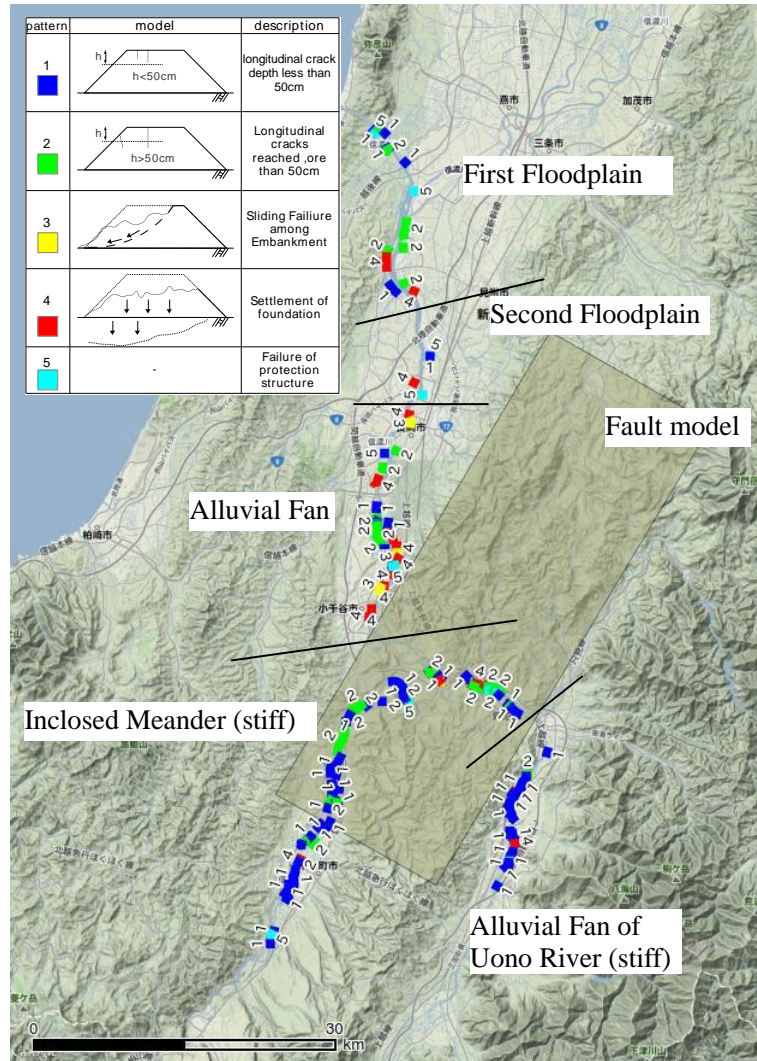


Fig.2 Location of intended damaged, non damaged levee and plan view of fault model. (map by Google Earth)

The damaged levees are shown in Fig. 2. The damage types were patterned into four types as shown in the legend of Fig. 2. The blue lines show pattern 1 (P1) which occurred shallow cracks on the levees, the green lines are pattern 2 (P2) which cracks on the levee reached over 50cm. The sliding failure of embankment is occurred in pattern 3 (P3) shown as yellow lines, and the settlement of embankment due to settlement of foundation is defined as pattern 4 (P4) of red lines. The pattern 5 (P5) shown as light blue line express the damage of structure.

First Floodplain region is placed on the downstream from 8 kilo-post of Shinano River, and the catastrophic failures P4 occurred as well as P2 with deep cracks as displayed in Fig. 2, although the most distant area from the epicenter and estimated fault model. The deep cracks may be related that the thick sand layer with high ground water level. That is, the saturated sand layer induced the liquefaction at the earthquake. And the P4 damage was occurred on the reclaimed ground.

In the Second Floodplain region, most of the levee has suffered no damages. It may be reason that the sand

layer is very thin and not saturated.

At the third region, Alluvial Fan Area, almost levees have insignificant damages, the foundation bellow the levee consists of the thick gravel with the enough strength. However, several short section levees, which are on the former river channel or near small channel, were suffered from significant damage. Such the geologically weak area may have caused the damage at the earthquake.

Around the fourth and fifth regions, where are near the epicenter, have stiff foundation such as bedrock. Therefore, almost damaged levees in these area had suffered only small cracks. The ground displacement in up-down direction was observed in the fourth region called Inclosed Meander Area, so the embankment protections made of concrete were damaged.

The fifth region of Alluvial Fan of Uono River is situated on bottom side of fault, and there were few ground displacement, then the levees and protection structures had only insignificant cracks.

## 2. Seismic Properties of Five Geological Regions and its Calculation Method

To obtain the seismic properties for five geological regions, two methods were explained in first. One is average dominant frequency,  $f_G$ , using one forth wave length law, such as the reciprocal of  $T_G$  in Specification of Highway Bridge in Japan. The other is dominant frequency,  $f_m$ , based on multiple reflection theory, and it can be consider the undulation of stiffness distribution for multiple layers, though the ground is assumed as elastic material.

The average dominant frequency,  $f_G$ , is obtained by following equations on multiple layers as shown in Fig. 3.

$$f_G = \frac{1}{4 \sum_{i=1}^n \frac{H_i}{V_{si}}} \quad (1a)$$

$$V_{si} = \sqrt{\frac{G_i}{\rho_i}} \quad (1b)$$

Where,  $H_i$  is depth of  $i$  th layer,  $G_i$  is shear modulus,  $\rho_i$  is wet density,  $h_i$  is damping constant and  $V_{si}$  is shear wave velocity.

The theoretical dominant frequency,  $f_m$ , is obtained from transfer function. The horizontal displacement,  $u_i(z_i, t)$ , in each layer are shown in Eq. (2a).

$$u_i(z_i, t) = U_i(z) e^{I\omega t} = (A_i e^{I\lambda_i z_i} + B_i e^{-I\lambda_i z_i}) e^{I\omega t} \quad (2a)$$

where  $I$  is imaginary unit,  $A_i$  and  $B_i$  are unknown constant.  $\lambda_i$  is expressed in Eq. (2b).

$$\lambda_i = \omega \sqrt{\frac{\rho_i}{G'_i}} \quad (2b)$$

where  $G'_i$  is called complex stiffness and defined as following formula.

$$G'_i = \left\{ 1 - 2h_{i2} + 2Ih_i \sqrt{1 - h_{i2}} \right\} G_i \quad (2c)$$

Equation (2c) is used so as to obtain same amplitude in hysteresis curvature. The boundary conditions of layer boundary continuity and zero shear stress on surface is substituted into Eq. (2a), then we

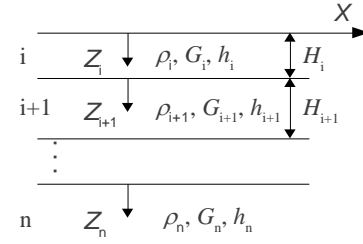


Fig.3 Multiple layers.

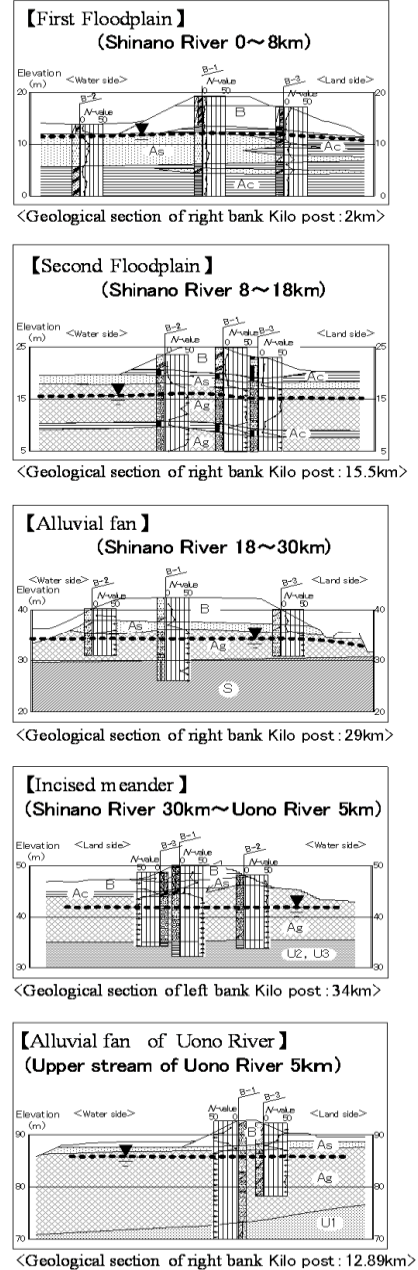
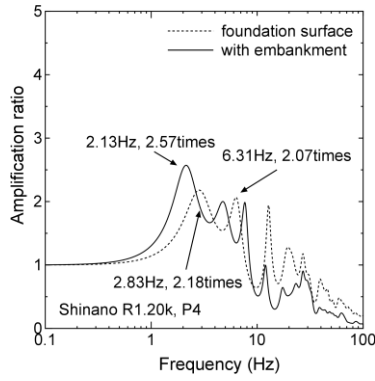
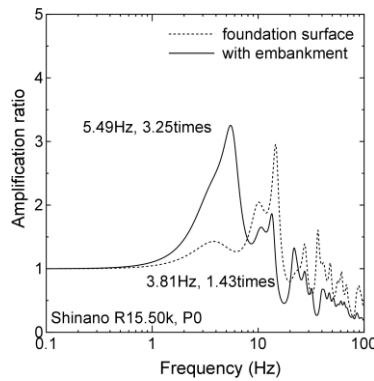


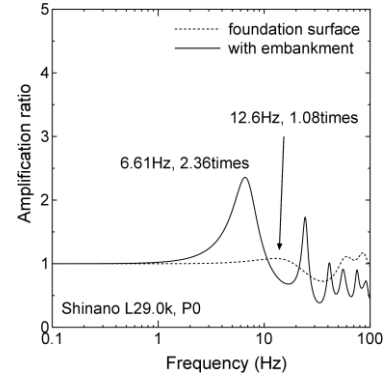
Fig.4 Typical soil profile for each geological regions.



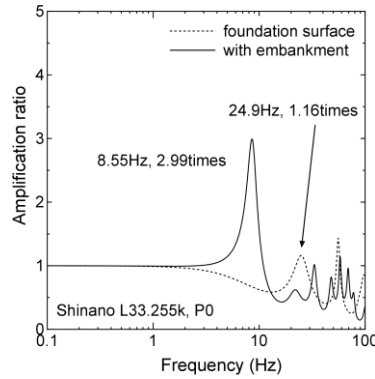
(a) First Floodplain.



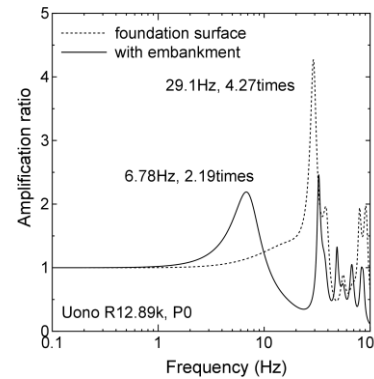
(b) Second Floodplain.



(c) Alluvial Fan.



(d) Inclosed Meander.



(e) Alluvial Fan of Uono River.

**Figs.5 (a)-(e)** Sample of transfer functions for each geological region.

obtained unknown constant  $A_i$  and  $B_i$  are expressed in recursive equation as follows.

$$\begin{cases} A_{i+1} = \frac{1}{2} A_i (1 + \alpha_i) e^{\nu_i H_i} + \frac{1}{2} B_i (1 - \alpha_i) e^{-\nu_i H_i} \\ B_{i+1} = \frac{1}{2} A_i (1 - \alpha_i) e^{\nu_i H_i} + \frac{1}{2} B_i (1 + \alpha_i) e^{-\nu_i H_i} \end{cases} \quad (3a)$$

where  $\alpha_i$  is defined in Eq. (3b).

$$\alpha_i = \frac{G'_i \lambda_i}{G'_{i+1} \lambda_{i+1}} \quad (3b)$$

The amplification ratio,  $R(\omega)$ , of ascending waves such as 2E/2E is expressed as in Eq. (3c).

$$R(\omega) = \left| \frac{2A_1}{2A_n} \right| \quad (3c)$$

The typical soil profiles for each region, which are classified in geological aspects, are shown in Fig. 4. The parameters for each layer were determined using results of standard penetration and laboratory soil tests. The average depth of calculation is about 25m from top of the embankment. Though it is difficult to determine the damping constant, the damping constant is estimated by observed data at NIGH01 of KiK-net, so as to fit the calculated surface response to observed acceleration wave. The estimated damping constant is shown in Table 2.

The densities of unmeasured layers are estimated with reference to measured density as shown in Table 3. The soil type is determined by soil profile in detail inspection of levee, although the stratum thickness of calculation model is not based on soil type. The thickness of each layer is one meter adapted to standard penetration test.

The samples of transfer function for the five geological region are shown in Figs. 5 (a)-(e). The dotted line

**Table 3** Definition of damping constant.

$V_s$ (m/s)	sand	clay
0~100	0.04	0.05
100~200	0.03	0.04
200~400	0.02	0.03
400~	0.01	0.02

**Table 4** Estimation of density which is unmeasured.

N Value	sand (g/cm <sup>3</sup> )	clay (g/cm <sup>3</sup> )
0~3	1.4	1.3
3~10	1.6	1.5
10~20	1.7	1.6
20~30	1.8	1.7
over 30	2.0	1.9
min. over 20m depth	1.8	1.7



shows the amplification ratio of foundation surface without embankment, and the solid line shows transfer function at the top of embankment. The first dominant frequency at embankment surface is smaller than the foundation among almost calculated points, this means embankment is weak compared with its foundation stratum.

### 2.1 Normalized Dominant Frequency by Peak Area of Transfer Function

The dominant frequency is determined by peak position of transfer function, however, there are plural peaks and the amplification ratio is also important in actual response. Even in the low dominant frequency, when the amplification ratio is very small, the response will be not so large. Therefore, to reflect these influences, the area around peak of transfer function as shown in Fig. 6 is considered.

The dominant frequency on the embankment in Fig.6 is  $f_m=5.3(\text{Hz})$ , and the area up to 20Hz and above 1.0 is shown as grayed hatch. The hatched area  $A$  is 13.4. The peak amplification ratio  $R=2.85$ . The proposing normalized dominant frequency,  $f_n$ , is expressed in Eq. (4).

$$f_n = \frac{f_m}{A/R} \quad (4)$$

For example, the normalized dominant frequency in Fig. 6,  $f_n=1.13$  (Hz).

Although the amplification ratio depends on the damping ratio which is difficult to be determined, the influences can be eliminated by dividing the area by the peak amplification ratio.

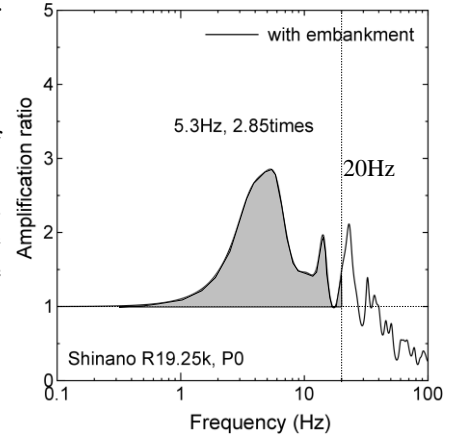
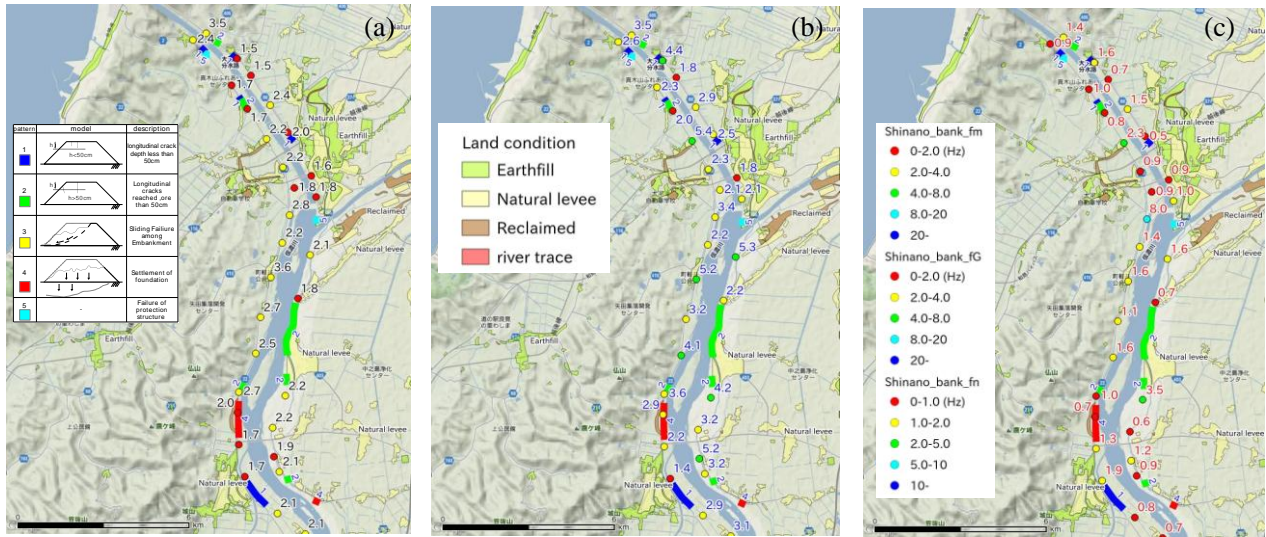


Fig.6 Peak area of transfer function

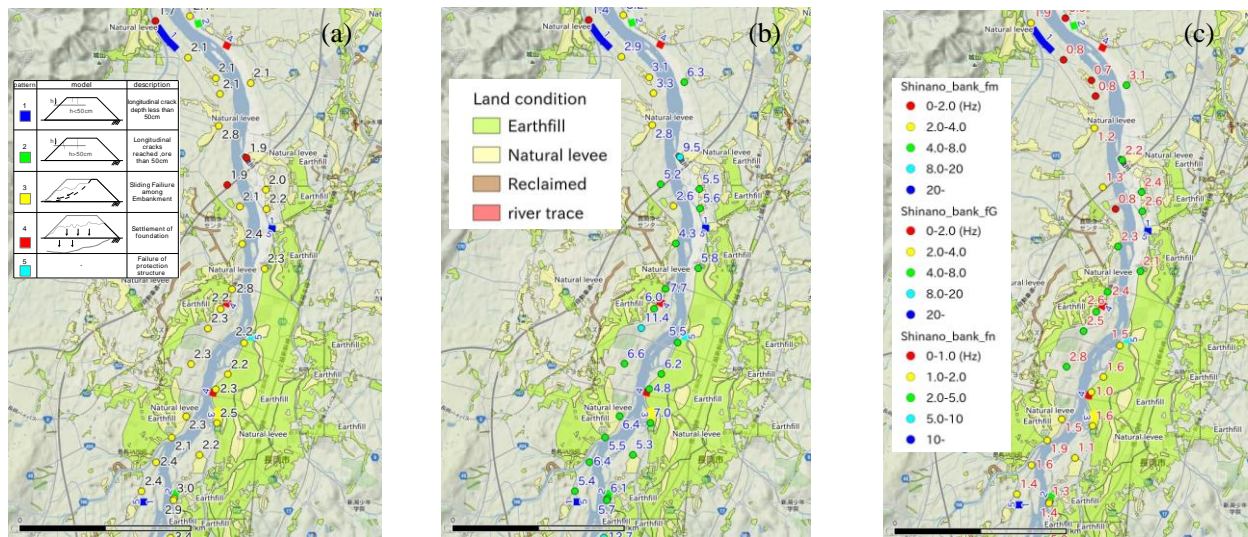
### 3. Comparison of Disaster Rank with Three Seismic Characteristics

The average dominant frequency  $f_G$ , theoretical dominant frequency by elastic model  $f_m$  and normalized frequency  $f_n$  are compared each other in Figs. 7 (a)-(c). The color coding by disaster pattern is mentioned in Fig.2, and the color classification is different between two dominant frequencies and the normalized frequency. When the frequency is lower, it is sound that the ground is weak, i.e. the color is yellow and red, for earthquake generally.

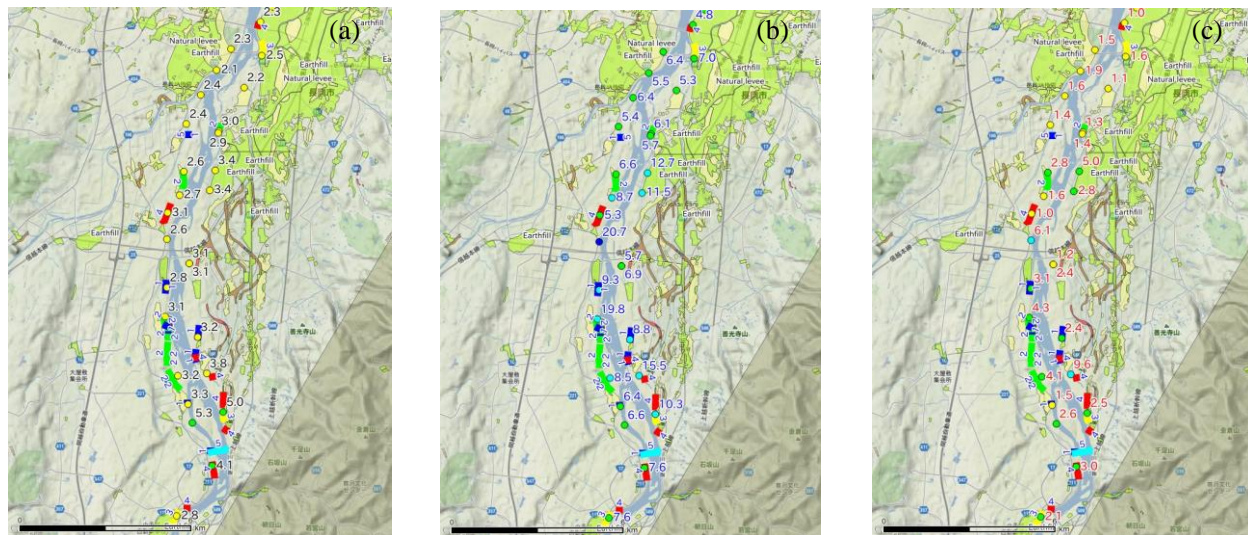
The general ground of first flood plain is very weak, then the differences of the three indexes are not so much, though the relationship shows  $f_m > f_g \gg f_n$ . Around the disaster pattern 4, the three seismic indexes show



Figs.7 (a)-(c) Comparison of seismic characteristic values with disaster pattern in First Flood Plain: (a)  $f_G$ , (b)  $f_m$ , (c)  $f_n$



**Figs.8 (a)-(c)** Comparison of seismic characteristic values with disaster pattern in Second Flood Plain: (a)  $f_G$ , (b)  $f_m$ , (c)  $f_n$



**Figs.9 (a)-(c)** Comparison of seismic characteristic values with disaster pattern in Alluvial Fan: (a)  $f_G$ , (b)  $f_m$ , (c)  $f_n$

red or yellow, however there are several points showing red in no damaged area. The P4 region is on the reclaimed ground, it is seemed to be available to adopt the multiple judgments of land condition and proposed seismic index.

The comparison of the indexes in second flood plain is shown in Figs.8 (a)-(c). The general ground properties become stiffer as indicated in Chapter 2. The relationship between the indexes are changed from the above, the  $f_m$  shows quite high compared with the others, i.e.  $f_m > f_g > f_n$ . It is found that the average dominant frequency is influenced soft ground around surface strongly. And the both of average and theoretical dominant frequencies are increased compared with the index values in first flood plain. However, the proposed normalized dominant frequency shows some lower values than in the first flood plain, and some higher values compared with the average frequencies.

The P4 failure, which is serious disaster for embankment, occurred in southern part of the Alluvial Fan as shown in Figs.9 (a)-(c). Some sites of P4 are near narrow canal, it might be consider that the high ground water level was enlarged their damages. The average of  $f_G$  and  $f_m$  are increased forward to upstream, and then those indexes even around P4 and P3 disaster are not so small, and the color is green. On the other hand, the  $f_n$  index can express the disaster level appropriately, the indexes around P4 disasters are enough low. At another point the normalized index shows high value, the influences of stiffer base ground condition is also expressed.



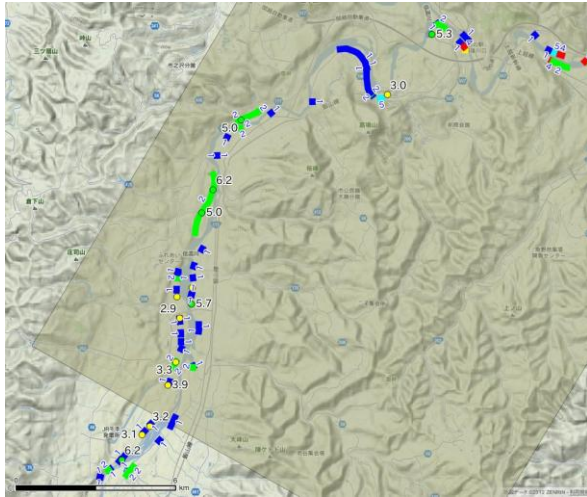


**Fig.9 (a)** Comparison of seismic characteristic of  $f_G$  with disaster pattern in Inclosed Meander

The Inclosed Meander area has stiff bed rock area, however this region is just on the fault model and nearest from epicenter. It seems that the average dominant frequency is underestimated compared with the theoretical frequency. And the index value of  $f_g$  on damaged levee due to deep cracks: P3 is higher than other small damaged area. The normalized frequency can express the P3 damages reasonably.

#### 4. Conclusions

To research available index for seismic damages of levee, we noted the dominant frequency of levee, the three types of dominant frequency were compared with actual damages of Shinano and Uono River on Niigata Chuetsu Earthquake in 2004.

From the results, the normalized dominant frequency, which is reduced the influences of damping ratio of ground, seems to be efficient index for seismic damages. The investigation of relationship between proposed seismic index and land use condition will be required to improve the accuracy.

#### Acknowledgments

The detail inspection data of Shinano River was provided by Shinano River and National Highway Office of MLIT. We show our gratitude to them.

#### References

- Sugimoto, T.: Relationship between Earthquake Damage of Embankment and Their Foundation, Geotechnical Engineering Magazine, Vol.59, No.2 Ser.No. 637, PP.20-23, 2011
- Shi, H. and Midorikawa, S.: New Attenuation Relationships for Peak Ground Acceleration and Velocity Considering Effects of Fault Type and Site Condition, Journal of Structural and Construction Engineering., Vol.523, pp.63-70, 1999.
- Sugimoto, T and Takahara, T, 2011, Relationship between Earthquake Damage Types of Levees and Seismic

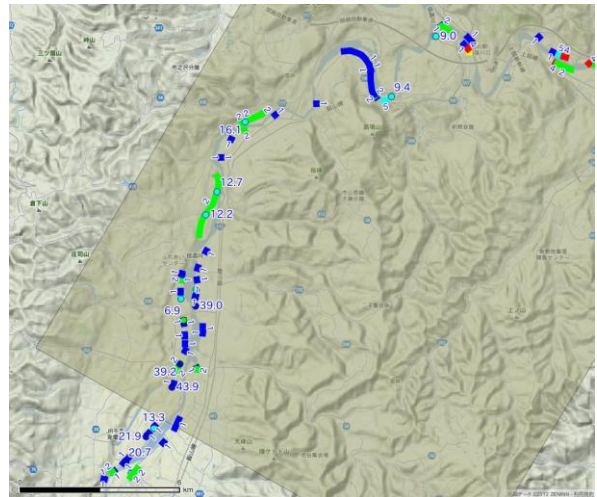


**Fig.9 (b)** Comparison of seismic characteristic of  $f_m$  with disaster pattern in Inclosed Meander

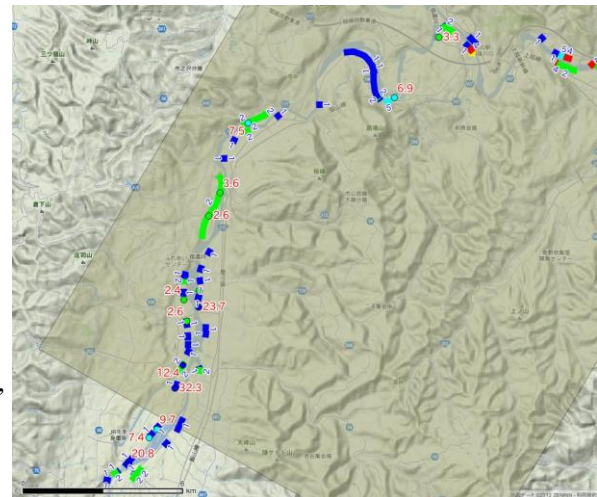


**Fig.9 (c)** Comparison of seismic characteristic of  $f_n$  with disaster pattern in Inclosed Meander

**T. Takahara**

Dept. of Civil Engineering, Faculty of Engineering.  
Kanazawa University, Japan  
Kakuma-machi, Kanazawa, Ishikawa, 920-1192, Japan  
e-mail: takahara@t.kanazawa-u.ac.jp

**T. Sugimoto**

MLIT Hokuriku Regional Development Bureau  
1-1-1, Misaki-cho, Chuo-ku, Niigata-shi, 950-8801, Japan  
e-mail : sugimoto-t8442@hrr.mlit.go.jp